Use of Genetic Algorithms in the Optimization of Free Radical Polymerizations Exhibiting the Trommsdorff Effect

S. S. S. CHAKRAVARTHY, D. N. SARAF, and SANTOSH K. GUPTA*

Department of Chemical Engineering, Indian Institute of Technology, Kanpur 208016, India

SYNOPSIS

The genetic algorithm (GA) is adapted and used to obtain optimal temperature histories for methyl methacrylate polymerizations. The reaction time is minimized, while simultaneously requiring the attainment of design values of the final monomer conversion and number average chain length. The technique is robust, and gives near-global optimal solutions. As such, it can easily be used for on-line optimizing control of free radical polymerization reactors in which the reaction is associated with the Trommsdorff effect. The results obtained from GA can be improved further if these are provided as initial guesses to a computer code using the Pontryagin minimum principle with the first order control vector iteration method. © 1997 John Wiley & Sons, Inc.

INTRODUCTION

A considerable amount of research has been reported in the last several years on the modeling and optimization of free radical polymerizations exhibiting the gel or the Trommsdorff effect.[1,2] The various models have been reviewed by O'Driscoll[3] and Hamielec[4] and more recently by Achilias and Kiparissides[5,6] and Mita and Horie.[7] These models have been used in several optimization studies, which have been reviewed by Farber,[8] as well as by Louie and Soong.[9] Yet, there are several unanswered questions. For example, Faldi et al.[10,11] have measured the diffusion coefficients of methyl methacrylate (MMA) and other model compounds in MMA–polymethyl methacrylate (PMMA) systems using forced Rayleigh scattering and field-gradient nuclear magnetic resonance (NMR) and have inferred that the propagation rate constant k_p (see Table I for the kinetic scheme) is not diffusion-controlled, contrary to the general assumption used in almost all theories. They claim that the decrease in k_p with increasing monomer conversion (x_m), which is necessary to fit experimental data on the rates of polymerization, needs an explanation different from the one traditionally being offered. Russell, Gilbert, and coworkers[12–14] are developing improved theories along similar lines. However, the earlier theories are fairly good and are still being used to model, optimize, and control industrial reactors, even though they are semi-empirical in nature.

One group of these theories has originated from the molecular theory of Chiu et al.[15] Chiu et al. relate the decrease of the rate constants, k_p and k_t, to the polymer concentration and the average molecular weight (the latter, through the initial concentration, $[I]_o$, of the initiator) at any time t. Achilias and Kiparissides[5,6] related some of the parameters of this early model to quantities that could be measured directly using nonpolymerizing systems. There was only a single curve-fit parameter, j_{co}, in their model, which was correlated to the initial value of the number average chain length, μ_{no}. The qualitative trends of the experimental data on the isothermal polymerization of MMA in small ampoules[16,17] (namely, sharp increase in x_m and the weight average chain length μ_w with t after the onset of the Trommsdorff effect, and the reaction stopping short of complete monomer conversion even though the reactions are irreversible, the latter being referred to as the glass

* To whom correspondence should be addressed.

Journal of Applied Polymer Science, Vol. 63, 529–548 (1997)
 CCC 0021-8995/97/040529-20

effect) were well explained by this theory, while quantitative agreement was ensured by curve-fitting the value of the parameter. One major drawback of these versions of this group of theories[5,6,15] was that they could not be applied to semibatch reactors or to reactors operating under non-isothermal conditions and so were of little use in industry where such operations were routinely encountered. Recently, Ray et al.[18] and Seth and Gupta[19] have presented a theory that relates the rate constants (as well as initiator efficiency[19] f) to the current values of the number average chain length μ_n. The parameters of this theory, θ_f, θ_p, and θ_t (all functions of temperature T) have been estimated[19] for MMA polymerization using the experimental data of Schulz and Harborth[16] and Balke and Hamielec,[17] under isothermal conditions in small ampoules. The theory so tuned has been able to explain quantitatively, experimental data on MMA polymerization in a 1 L PC-interfaced, stainless steel, Parr® reactor using idealized conditions mimicking industrial operations (namely, step changes in temperature[20] and step increases in the initiator and monomer concentrations[21]). No additional retuning of the parameters was found to be necessary. This suggests that the theory reflects all the physicochemical phenomena associated with polymerization quite well. It is to be noted that other groups of theories could have been modified suitably to apply to industrial systems, but it is well recognized[22] that almost all theories are about equally successful in explaining rate data, and so the use of the relatively simple and continuous models in the group originating from Chiu et al.[15] is justified.

In this work, the recent theory[18,19] for MMA polymerization has been used to study the optimization of a batch reactor. A commonly studied problem[8,9] is to obtain the temperature history $T(t)$ (the control variable), which minimizes the total reaction time t_f, while simultaneously requiring the final monomer conversion x_{mf} and the final value of the number average chain length μ_{nf} to meet certain specifications (called desired values, x_{md} and μ_{nd}). This ensures economic operation, as well as some product property requirements, and is referred to as the minimum-time problem.[8] Another common optimization problem [minimum polydispersity index (PDI) problem] is to minimize the PDI of the polymer product. Unfortunately, it is quite difficult to satisfy all of these requirements (min t_f, min PDI, $\mu_{nf} = \mu_{nd}$, $x_{mf} = x_{md}$) simultaneously.[8] Our choice of the minimum time problem can be faulted for having some kind of an academic bias. However, the techniques developed herein are quite general and are applicable to the minimum PDI (or any other) optimization problem.

A newly emerging technique, called genetic algorithm (GA),[23–25] has been used to obtain optimal solutions. This is an extremely robust technique and gives solutions that are quite close to global optimum, reasonably fast. Hence, this technique, coupled with a model that is applicable for industrial reactors, is well suited for use for on-line optimizing control of large scale MMA polymerizations (or of other similar free radical polymerizations), provided we can estimate the state of the system on-line. Current experimental work along these lines is in progress, in which the viscosity of the reaction mass is used for inferential state estimation.[26,27] GA will then be used to predict the optimal trajectory of future control actions (reactor temperature will be used as the control variable) at the supervisory level. The actual implementation of the control on the reactor will be effected through a front-end controller. In the present investigation, use of GA has been restricted to generate open-loop optimal temperature histories of the polymerization reactor.

Most of the earlier works[8] on the optimization of polymerization reactors use the far less robust Pontryagin's minimum principle[27–30] or the constrained pattern search technique[9] to solve a variety of optimization problems as described in the review of Farber,[8] using temperature or initiator addition rates as control variables. These techniques are not suitable for use for on-line optimization work. GA, on the other hand, is a new and extremely powerful search technique based on the mechanics of natural genetics and natural selection. This algorithm was introduced in the mid 1960s by Holland;[23]a discussion of the technique and its adaptations, as well as its major applications, are available in several books.[24,25] It involves a random search over the control variable domain after the problem has been appropriately coded, usually in terms of strings or chromosomes comprising binary numbers. The best few solutions evolve over generations using techniques that mimic genetic evolution (hence, the name). This new technique has been proved to be very efficient, especially in cases in which the objective function is flat and exhibits several local optima. The advantage of GA lies in the fact that it works without requiring much information about the system, in contrast to the traditional techniques, which need gradients, initial guesses, etc. Hence,

Table I Kinetic Scheme for Polymerization of MMA

Initiation	$I \xrightarrow{k_d} 2R$
	$R + M \xrightarrow{k_i} P_1$
Propagation	$P_n + M \xrightarrow{k_p} P_{n+1}$
Termination by combination	$P_n + P_m \xrightarrow{k_{tc}} D_{n+m}$ $(k_{tc} \cong 0$ for MMA)
Termination by disproportionation	$P_n + P_m \xrightarrow{k_{td}} D_n + D_m$
Chain transfer to monomer	$P_n + M \xrightarrow{k_f} P_1 + D_n$
Chain transfer to monomer via solvent	$P_n + S \xrightarrow{k_s} S^{\cdot} + D_n$
	$S^{\cdot} + M \xrightarrow{\text{fast}} S + P_1$
	or
	$P_n + M \xrightarrow{k_s} D_n + P_1$

for more complex systems, in which the gradients cannot be easily evaluated and the initial guess becomes crucial, GAs lead to solutions that are very close to the global optimum or, in fact, provide very good initial points to start off other techniques that require excellent initial guesses (e.g., Pontryagin's minimum principle using the first order control vector iteration method).

FORMULATION

Table I gives the kinetic scheme for MMA polymerization (with $k_{tc} \simeq 0$). The mass balances for MMA polymerization in a semibatch reactor are given by equations having the general form

$$d\boldsymbol{x}/dt = \boldsymbol{F}(\boldsymbol{x}, \boldsymbol{u}); \quad \boldsymbol{x}(t = 0) = \boldsymbol{x}_o \qquad (1)$$

where $\boldsymbol{x}(t)$ is the vector of state variables defined by

$$\boldsymbol{x} \equiv [I, M, R, S, \lambda_0, \lambda_1, \lambda_2, \mu_0, \mu_1, \mu_2, \zeta_m, \zeta_{m1}]^T \qquad (2)$$

and $\boldsymbol{u}(t)$ is the vector of control variables [in the present case, it is a scalar $T(t)$]:

$$\boldsymbol{u}(t) = u(t) = T(t) \qquad (3)$$

λ_k and μ_k ($k = 0, 1, 2, \cdots$) represent the kth moments of the chain length distributions of species P_n and D_n, respectively. ξ_m, ξ_{m1} are additional variables to account for addition and vaporization of monomer after time $t = 0$ and are useful in the definition of the monomer conversion x_m for semibatch reactors. The other symbols are defined in the nomenclature section. The (general) mass balance and moment equations [functions, $\boldsymbol{F}$, in eq. (1)] have been given by Ray et al.,[18] as well as by Seth and Gupta,[19] and are given in Table II, along with related expressions for the rate constants, accounting for diffusional limitations exhibited at higher monomer conversions. Table III gives the values of the several properties and parameters to be used for MMA polymerization.

Equations (a)–(c) in Table II express the initiator efficiency f and the rate constants k_p and k_{td} ($=k_t$ for PMMA) in the following form:

$$f = f(\boldsymbol{x}, u, \boldsymbol{p}) \qquad (4a)$$

$$k_p = k_p(\boldsymbol{x}, u, \boldsymbol{p}) \qquad (4b)$$

$$k_{td} = k_{td}(\boldsymbol{x}, u, \boldsymbol{p}) \qquad (4c)$$

with

$$\boldsymbol{p} = [\theta_f, \theta_p, \theta_t]^T \qquad (5)$$

More details can be found in Ray et al.[18] and Seth and Gupta.[19] The model parameters θ_f, θ_p, and θ_t have been tuned using the isothermal data of Balke and Hamielec[17] on MMA polymerization in small ampoules. The model has been found to be in good agreement with the experimental data on a 1 L Parr® reactor.[20,21] No retuning of the values of the parameters $\boldsymbol{p}$ were found to be necessary.

The objective function I used in this study is given by

Table II Model Equations for MMA Polymerization in Semibatch Reactors[a]

Mass Balance and Moment Equations

1. $\dfrac{dI}{dt} = -k_d I + R_{li}(t)$
2. $\dfrac{dM}{dt} = -(k_p + k_f)\dfrac{\lambda_o M}{V_l} - k_i \dfrac{RM}{V_l} - k_s S \dfrac{\lambda_o}{V_l} + R_{lm}(t) - R_{vm}(t)$
3. $\dfrac{dR}{dt} = 2fk_d I - k_i \dfrac{RM}{V_l}$
4. $\dfrac{dS}{dt} = R_{ls}(t) - R_{vs}(t)$
5. $\dfrac{d\lambda_o}{dt} = k_i \dfrac{RM}{V_l} - k_t \dfrac{\lambda_o^2}{V_l}$
6. $\dfrac{d\lambda_1}{dt} = k_i \dfrac{RM}{V_l} + k_p M \dfrac{\lambda_o}{V_l} - k_t \dfrac{\lambda_o \lambda_1}{V_l} + (k_s S + k_f M)\dfrac{(\lambda_o - \lambda_1)}{V_l}$
7. $\dfrac{d\lambda_2}{dt} = k_i \dfrac{RM}{V_l} + k_p M \dfrac{\lambda_o + 2\lambda_1}{V_l} - k_t \dfrac{\lambda_o \lambda_2}{V_l} + (k_s S + k_f M)\dfrac{(\lambda_o - \lambda_2)}{V_l}$
8. $\dfrac{d\mu_o}{dt} = (k_s S + k_f M)\dfrac{\lambda_o}{V_l} + \left(k_{td} + \dfrac{1}{2}k_{tc}\right)\dfrac{\lambda_o^2}{V_l}$
9. $\dfrac{d\mu_l}{dt} = (k_s S + k_f M)\dfrac{\lambda_1}{V_l} + k_t \dfrac{\lambda_o \lambda_1}{V_l}$
10. $\dfrac{d\mu_2}{dt} = (k_s S + k_f M)\dfrac{\lambda_2}{V_l} + k_t \dfrac{\lambda_o \lambda_2}{V_l} + k_{tc}\dfrac{\lambda_1^2}{V_l}$
11. $\dfrac{d\xi_m}{dt} = R_{lm}(t) - R_{vm}(t)$
12. $\dfrac{d\xi_{m_l}}{dt} = R_{lm}(t)$
13. $V_l = \dfrac{S(MW_s)}{\rho_s} + \dfrac{M(MW_m)}{\rho_m} + \dfrac{(\xi_m - M)(MW_m)}{\rho_p}$
14. $\phi_m = \dfrac{M(MW_m)/\rho_m}{\dfrac{M(MW_m)}{\rho_m} + \dfrac{S(MW_s)}{\rho_s} + \dfrac{(\xi_m - M)(MW_m)}{\rho_p}}$
15. $\phi_s = \dfrac{S(MW_s)/\rho_s}{\dfrac{M(MW_m)}{\rho_m} + \dfrac{S(MW_s)}{\rho_s} + \dfrac{(\xi_m - M)(MW_m)}{\rho_p}}$
16. $\phi_p = 1 - \phi_m - \phi_s$

$$\text{Min } I[u(t)] = t_f + w_1(1 - x_{mf}/x_{md})^2 + w_2(1 - \mu_{nf}/\mu_{nd})^2 \quad (6a)$$

subject to (s.t.)

$$d\boldsymbol{x}/dt = \boldsymbol{F}(\boldsymbol{x}, u) \quad (6b)$$

$$u_{\min} \le u(t) \le u_{\max} \quad (6c)$$

where

$$x_m(t) \equiv (1 - M/\zeta_{m1}) \quad (7a)$$

$$\mu_n(t) = (\lambda_1 + \mu_1)/(\lambda_o + \mu_o) \quad (7b)$$

$$x_{mf} = x_m(t_f) \quad (7c)$$

$$\mu_{nf} = \mu_n(t_f) \quad (7d)$$

In eq. (6), x_{md} and μ_{nd} are the desired values of monomer conversion; and the number average chain length at $t = t_f$, x_{mf}, and μ_{nf} are the actual values corresponding to $t = t_f$, and w_1 and w_2 are (large) weightage factors. The choice of the objective function in eq. (6) minimizes the deviations (due to large values of w_1 and w_2) of x_{mf} and μ_{nf} from their desired values. The form of I used in eq. (6) in which the end point requirements (constraints) are included as penalty functions is quite popular.[8,25] The choice, $x_{mf} \cong x_{md}$, forces the amount of unreacted monomer to be small, thus keeping post-reactor separation and recycling costs low. The choice, $\mu_{nf} \cong \mu_{nd}$, forces the polymer properties to be as per

Table II Continued

Cage, Gel, and Glass Effect Equations

$$\frac{1}{f} = \frac{1}{f_o}\left[1 + \theta_f(T)\,\frac{M}{V_l}\,\frac{1}{\exp\,[\xi_{I3}\{-\psi + \psi_{\text{ref}}\}]}\right] \tag{a}$$

$$\frac{1}{k_t} = \frac{1}{k_{t,o}} + \theta_t(T)\,\mu_n^2\,\frac{\lambda_o}{V_l}\,\frac{1}{\exp[-\psi + \psi_{\text{ref}}]} \tag{b}$$

$$\frac{1}{k_p} = \frac{1}{k_{p,o}} + \theta_p(T)\,\frac{\lambda_o}{V_l}\,\frac{1}{\exp[\xi_{13}\{-\psi + \psi_{\text{ref}}\}]} \tag{c}$$

$$\psi = \frac{\gamma\left\{\dfrac{\rho_m\phi_m\hat{V}_m^*}{\xi_{13}} + \dfrac{\rho_s\,\phi_s\hat{V}_s^*}{\xi_{23}} + \rho_p\,\phi_p\hat{V}_p^*\right\}}{\rho_m\phi_m\hat{V}_m^*V_{fm} + \rho_s\phi_s\hat{V}_s^*V_{fs} + \rho_p\phi_p\hat{V}_p^*V_{fp}} \tag{d}$$

$$\psi_{\text{ref}} = \frac{\phi}{V_{fp}} \tag{e}$$

$$\xi_{13} = \frac{\hat{V}_m^*(MW_m)}{\hat{V}_p^*M_{jp}} \tag{f}$$

$$\xi_{23} = \frac{\hat{V}_s^*(MW_s)}{\hat{V}_p^*M_{jp}} \tag{g}$$

$$\xi_{I3} = \frac{\hat{V}_I^*(MW_I)}{\hat{V}_p^*M_{jp}} \tag{h}$$

$$k_d = k_d^o\,\exp(-E_d/RT) \tag{i}$$

$$k_{p,o} = k_{p,o}^o\,\exp(-E_p/RT) \tag{j}$$

$$k_{t,o} = k_{td,o} = k_{td,o}^o\,\exp(-E_{td}/RT) \tag{k}$$

[a] Refer to Seth and Gupta.[19]

specifications, since several physical properties of polymers are related to the value of their μ_n. The objective function in eq. (6) has been used earlier by Sachs et al.,[31] but with a different kinetic model, and by Farber and Laurence[32] for styrene polymerization. The techniques developed herein are quite general and can be applied to other choices of the objective function and end-point constraints (as well as to low molecular weight systems). The initial values $\boldsymbol{x}_o$ in eq. (1) are given by

$$\boldsymbol{x}_o = [I_o,\, M_o,\, 0,\, 0,\, 0,\, 0,\, 0,\, 0,\, 0,\, 0,\, M_o,\, M_o]^T \tag{8}$$

Figure 1 gives the flow chart illustrating how GA, as applied to the present problem [eq. (6)] works. We have had to make several adaptations to the conventional algorithm[24,25] and the computer code (SGA[25]) in order to solve the present problem. Initially (at generation number $N_g = 0$), a population having N_p chromosomes, $l_{N_{\text{chr}}}^{(i)}$; $i = 1, 2, \ldots, N_p$, is generated. Each chromosome in this population comprises of a sequence of N_{ga} numbers (called substrings), which are binary representations of values of the control variable at N_{ga} equispaced points in $0 \le t \le t_{fo}$ (t_{fo}, an initial estimate of t_f, is to be supplied). Each of these substrings, in turn, comprises of a set of N_{str} binary numbers (0 or 1). Thus, each chromosome has $N_{\text{chr}} \equiv N_{\text{ga}}N_{\text{str}}$ binary digits. The N_{chr} individual binaries are generated using a random number generator subroutine. The binary string (sequence of N_{chr} binaries) of the i^{th} chromosome, when decoded and interpolated (mapped) between the upper ($u \le b$) and lower ($u \ge a$) bounds of u, gives a digitized u-history (a set of N_{ga} values), $[u^{(i)}] \equiv [u^{(i)}(1), u^{(i)}(2), \ldots, u^{(i)}(N_{\text{ga}})]$, corresponding to that chro-

Table III Parameters Used for Polymerization of MMA

ρ_m = 966.5 − 1.1 (T − 273.1) kg/m^3
ρ_p = 1200 kg/m^3
ρ_s = 844.18 − 1.07165 (T − 323.1) kg/m^3 (benzene)
f_o = 0.58; for AIBN
f_o = 1.00; for BPO
k_d^o = 1.69 × 10^{14} s^{-1}; for BPO
k_d^o = 1.053 × 10^{15} s^{-1}; for AIBN
$k_{p,o}^o$ = 4.917 × 10^2 m^3/mol-s
$k_{td,o}^o$ = 9.8 × 10^4 m^3/mol-s
k_{tc} = 0.0
k_f = 0.0
k_i = k_p
k_s = 0.0
E_d = 125.40 kJ/mol; from BPO
E_d = 128.45 kJ/mol; for AIBN
E_p = 18.22 kJ/mol
E_{td} = 2.937 kJ/mol
(MW_m) = 0.10013 kg/mol
(MW_s) = 0.07811 kg/mol
(MW_I) = 0.06800 kg/mol; for radicals from AIBN
(MW_I) = 0.07700 kg/mol; for radicals from BPO

Constitutive Parameters for the Cage, Gel, and Glass Effects
$\hat{V}_I^*$ = 9.13 × 10^{-4} m^3/kg; for AIBN
$\hat{V}_I^*$ = 8.25 × 10^{-4} m^3/kg; for BPO
$\hat{V}_m^*$ = 8.22 × 10^{-4} m^3/kg
$\hat{V}_p^*$ = 7.70 × 10^{-4} m^3/kg
$\hat{V}_s^*$ = 9.01 × 10^{-4} m^3/kg; for benzene
M_{jp} = 0.18781 kg/mol
γ = 1
V_{fm} = 0.149 + 2.9 × 10^{-4} [$T(K)$ − 273.1]
V_{fp} = 0.0194 + 1.3 × 10^{-4} [$T(K)$ − 273.1 − 105]; for $T < (105 + 273.1)\ K$
V_{fs} = 0.025 + 1.0 × 10^{-3} [$T(K)$ − 171.1] (benzene)

Best-fit Correlations (BFCs)
$\log_{10}[\theta_t(T), s]$ = 1.241 × 10^2 − 1.0314 × 10^5 (1/T) + 2.2735 × 10^7 (1/T^2)
$\log_{10}[\theta_p(T), s]$ = 8.03 × 10^1 − 7.50 × 10^4 (1/T) + 1.765 × 10^7 (1/T^2)

For AIBN–MMA system (bulk polymerization):
$\log_{10}[10^3\theta_f(T), \text{m}^3\ \text{mol}^{-1}]$ = 2.016 × 10^2 − 1.455 × 10^5 (1/T) + 2.70 × 10^7 (1/T^2)

For BPO–benzene–MMA system (solution polymerization):
$\log_{10}[10^3\theta_f(T), \text{m}^3\ \text{mol}^{-1}]$ = −3.763 × 10^1 + 1.686 × 10^4 (1/T)

mosome, as described in Table IV (in the conventional GA,[24,25] $b = u_{\max}$ and $a = u_{\min}$). At this stage, we have a set of N_p chromosomes, each representing a different digitized $u(t)$ history, appropriately coded in the form of a string of N_{chr} binaries. The minimum difference between any two digitized values of u is $(b - a)/(2^{N_{str}} - 1)$, this being the accuracy to which u can be determined.

The values of $u^{(i)}(j)$ generated by the above procedure using $b = u_{\max}$ and $a = u_{\min}$ could fluctuate wildly between these two limits. This leads to significant oscillations in the optimal u histories and is both undesirable and non-implementable. In order to reduce these oscillations, further constraints are clamped on to the values of $u^{(i)}(j)$ in the present study so that neighboring values of u do not differ by more than some prescribed values, $\Delta u_{\min}$ and $\Delta u_{\max}$. Thus,

$$\Delta u_{\min} \le \Delta u^{(i)}(j)[\equiv u^{(i)}(j+1) - u^{(i)}(j)] \le \Delta u_{\max} \quad (9)$$

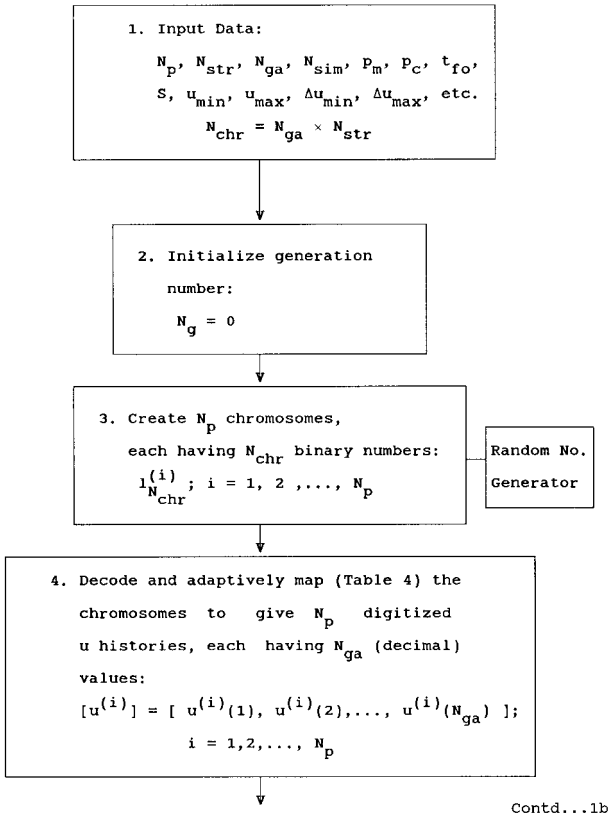

Fig. 1 Flowchart indicating the working of GA.

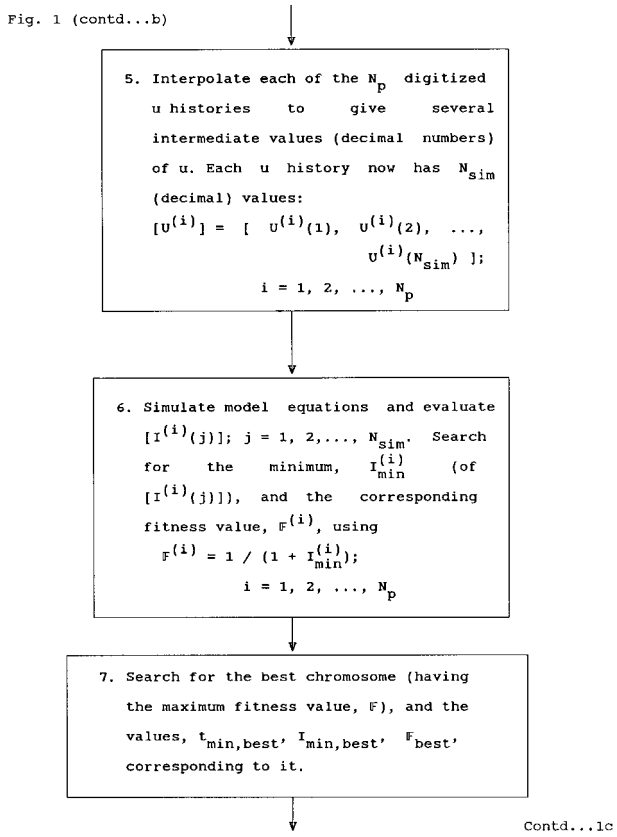

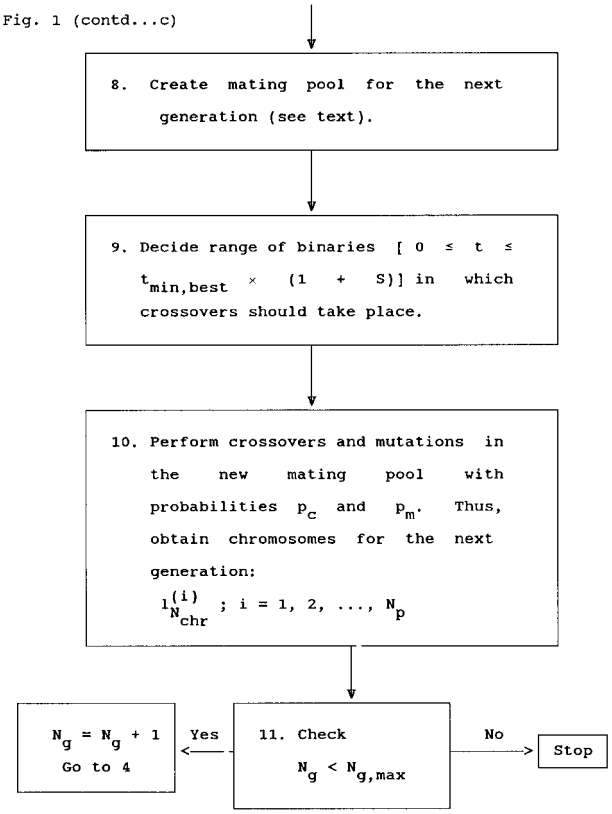

Figure 1 Flow chart indicating the working of GA.

or

$$u^{(i)}(j) + \Delta u_{\min} \leq u^{(i)}(j+1) \leq u^{(i)}(j) + \Delta u_{\max} \quad (10)$$

where $\Delta u_{\min}$ is a negative number. Thus, the first value, $u^{(i)}(1)$, corresponding to $t = 0$ is determined randomly to lie between $u_{\max}$ and $u_{\min}$, while all subsequent values are determined randomly within a smaller range around the previous value. This procedure is being called adaptive mapping. The accuracy (minimum difference between values of u) of internal points is observed to be higher than for the first ($t = 0$) point, if $|\Delta u_{\max} - \Delta u_{\min}| < |u_{\max} - u_{\min}|$.

The decoded and adaptively mapped, discretized values of u are curve-fitted piece-wise (splines) to obtain a continuous function, $u^{(i)}(t)$. A piece-wise cubic Hermite subroutine is used to do this. This continuous function is again digitized to give N_{sim} ($\geq N_{\text{ga}}$) values of the control variable, $[U^{(i)}(j); j = 1, 2, \ldots, N_{\text{sim}}]$. The generation of several additional intermediate, discretized values of $u^{(i)}$ is necessary for integrating the model differential equations [eq. (1)].

The digitized temperature history, $[U^{(i)}(j); j = 1, 2, \ldots, N_{\text{sim}}]$, corresponding to the i^{th} member of the population, is used in a Gear subroutine[33] (D02EJF in the NAG library) to integrate the balance equations, starting with the initial conditions in eq. (8) and continuing until $t = t_{fo}$. The program stores the values of each of the state variables, $\boldsymbol{x}^{(i)}(j)$, at every intermediate value of t, such that there are N_{sim} sets of $\boldsymbol{x}$. The value of $I^{(i)}$ at each of these storage locations is computed, and the location $t^{(i)}_{\min}$ of the minimum of $I^{(i)}$, as well as the minimum value itself, $I^{(i)}_{\min}$, are obtained by search. Evidently, t_{fo} should be chosen large enough so that $I_{\min}$ occurs in $0 \leq t \leq t_{fo}$ for all i. The integration of the balance equations and the location of $I^{(i)}_{\min}$ for each of the N_p chromosomes is carried out.

One additional point needs to be emphasized. The computer code SGA,[25] which has been used in this study after modification maximizes a fitness function $\mathbb{F}^{(i)}$ rather than minimizes an objective function I. Hence, we define a fitness function as follows:

$$\mathbb{F}^{(i)} \equiv 1/(1 + I^{(i)}_{\min}) \quad (11)$$

and maximize its value (wherever $I^{(i)}$ is to be minimized).

The next step in GA is to have reproduction in the population of chromosomes. A mating pool is first formed. In this pool, priority is given to those chromosomes that have higher fitness values. The essential idea is to pick out the above average strings in the current population and include (multiple) copies of these in the mating pool in a probabilistic manner. It is here that the principle of natural selection (survival of the fittest) comes in action. The principle of proportionate reproduction is used. The probability of selecting the i^{th} chromosome in the mating pool is $\mathbb{F}^{(i)}/\sum_{i=1}^{N_p} \mathbb{F}^{(i)}$. A roulette wheel (whose circumference is marked for each chromosome proportionate to its fitness value) is spun N_p times. In each spin, the chromosome corresponding to the location of the roulette wheel pointer is copied into the pool. This thought experiment is implemented using N_p random numbers.[24,25]

After the mating pool is created, crossover and mutations take place to produce the new population (next generation). These operations take place at the chromosome (binary) level. Two chromosomes are selected randomly from the mating pool, a crossing site is selected (randomly again), and portions of the chromosomes before and after the crossing site are exchanged. For example, for seven-bit chromosomes with crossing site after the third binary, the crossover is described by the following:

Table IV Decoding and Adaptive Mapping Procedure for $N_{ga} = 2$

$N_{\text{chr}} = N_{ga}N_{\text{str}} = 2N_{\text{str}}$; $a \leq u \leq b$[a]

Example:

$l^{(i)}_{N_{\text{chr}}} = [10011\cdots0; 11100\cdots0]; \quad i = 1, 2, \ldots, N_p$

N_{str} binaries N_{str} binaries

Decode each of the (two sets of) binary numbers into decimal numbers, d_1 and d_2, using, for example,

$$d_1 = 1 \times 2^{N_{\text{str}}-1} + 0 \times 2^{N_{\text{str}}-2} + \cdots + 0 \times 2^0$$

Now, using the mapping, obtain the digitized u history

$$[u^{(i)}(j)] = [u^{(i)}(1), u^{(i)}(2)] = a + d_j \times \text{VAL}; \quad i = 1, 2, \ldots, N_p; \quad j = 1, 2$$

where

$$\text{VAL} = (b - a)/2^{N_{\text{str}}} - 1)$$

[a] $a = u_{\min}$, $b = u_{\max}$; for $j = 1$ $a = u_{(i)}(j-1) + \Delta u_{\min}$, $b = u^{(i)}(j-1) + \Delta u_{\max}$; for $j > 1$; s.t. $u_{\min} \leq a, b \leq u_{\max}$

$$\begin{array}{l} 100|1111 \\ 110|0100 \end{array} \rightarrow \begin{array}{ll} 100 & 0100 \\ 110 & 1111 \end{array}$$

(old generation) (new generation) (12)

While performing crossovers, only $N_p p_c$ chromosomes are crossed, the remaining being left untouched (p_c is referred to as the crossover probability).

Another operation, called mutation, is also used to improve the next generation. The mutation operator changes a binary number from 1 to 0 or vice versa, with a probability p_m. This operation is carried out for each of the $N_p N_{\text{chr}}$ bits in the population, again using appropriate random numbers.[24,25] The need for mutation leads to a local search around the current solution and helps maintain the diversity of the population.[25]

The random crossover procedure discussed above leads to a preponderance of crossovers in the (inactive) range, $t_{\min}^{(i)} \leq t \leq t_{fo}$, if the guess value of t_{fo} supplied to the computer code is too large. This procedure thus needs to be adapted so that crossovers take place in a t-domain (horizon), which becomes smaller over generations. What is done is to limit crossovers to $0 \leq t \leq t_{\min,\text{best}} \times (1 + S)$, where $t_{\min,\text{best}}$ is the best (minimum) of the N_p values of $t_{\min}^{(i)}$ in any generation, and S is a safety factor supplied to the program (obtained by numerical experimentation). The string length corresponding to $t_{\min,\text{best}}(1 + S)$ is given by

$$N'_{\text{chr}} = N_{\text{chr}} t_{\min,\text{best}}(1 + S)/t_{fo} \qquad (13)$$

where N'_{chr} is an (next higher) integer. The region in which crossovers take place would decrease from generation to generation as $t_{\min,\text{best}}$ decreases. Such an adaptation of the conventional GA can be used to advantage for any minimum time optimization problem and provides an automatically narrowing crossover horizon.

The optimal solutions generated using GA can be compared with those obtained (for the same objective function, constraints, and model equations) from Pontryagin's minimum principle[27–30] using the first order control vector iteration technique (referred to as P1). The algorithm used is summarized in Table V and is an adaptation of that used by Vaid and Gupta[34] and Ray and Gupta[35] earlier.

Table V Formulation of the Optimal Control Problem Using Pontryagin's Minimum Principle[a] With First Order Control Vector Iteration Method

Optimization Problem

$$\begin{aligned} &\text{Max } I[u(t)] = G[\boldsymbol{x}(t_f)] \\ &\text{s.t.} \\ &\quad d\boldsymbol{x}/dt = \boldsymbol{F}(\boldsymbol{x}, u) \\ &\quad u_{\min} \leq u(t) \leq u_{\max} \end{aligned}$$

Here,

$$G[\boldsymbol{x}(t_f)] = -[t_f + w_1(1 - x_{mf}/x_{md})^2 + w_2(1 - \mu_{nf}/\mu_{nd})^2]$$

Procedure

1. Guess $u(t) = T^{(o)}(t)$; $0 \leq t \leq t_{fo}$
2. With this $u(t)$, integrate the state variable equations $d\boldsymbol{x}/dt = \boldsymbol{F}(\boldsymbol{x}, u)$ to obtain $\boldsymbol{x}(t)$; $0 \leq t \leq t_f$, with t_f obtained by solving
$$H(t_f) = (\partial G/\partial \boldsymbol{x})\boldsymbol{F}|_{t=t_f} = 0$$
3. With the values of $\boldsymbol{x}(t)$ and $u(t)$, integrate the adjoint equations backwards from $t = t_f$ to $t = 0$,
$$d\boldsymbol{\lambda}^T/dt = -(\partial H/\partial \boldsymbol{x}); \; \boldsymbol{\lambda}^T(t_f) = \partial G/\partial \boldsymbol{x}\,|_{t=t_f}$$
where $H = \boldsymbol{\lambda}^T \boldsymbol{F}$
4. Correct $u(t)$ by
$$u(t) = u(t) + \varepsilon(\partial H/\partial u), \quad \varepsilon > 0$$
5. Perform a single variable search (on ε) to generate several $u(t)$, obtain I for each of these histories (after integrating the state variable equations for each case), then obtain ε_{opt} corresponding to the maximum value of I (note that $\partial H/\partial u$ is not updated during this search).
6. Update $u(t)$ by
$$u^{\text{new}}(t) = u^{\text{old}}(t) + \varepsilon_{\text{opt}}(\partial H/\partial u)$$
and return to step 2.
7. Iterate until convergence is attained.

[a] Refer to Ray, Ray and Szekeley, Bryson and Ho, and Lapidus and Luus.[27–30]

RESULTS AND DISCUSSION

Several checks were made to ensure that the computer code prepared was free of errors. The code was used to generate the monomer conversion and the number average chain length for different isothermal conditions. These were found to match the results of Seth and Gupta[19] and are shown in Figure 2 for an initial initiator concentration $[I]_o$ of 25.8 mol/m^3 (reference value). These results were generated with a value of TOL of 10^{-7} in the code DO2EJF, and no significant differences were

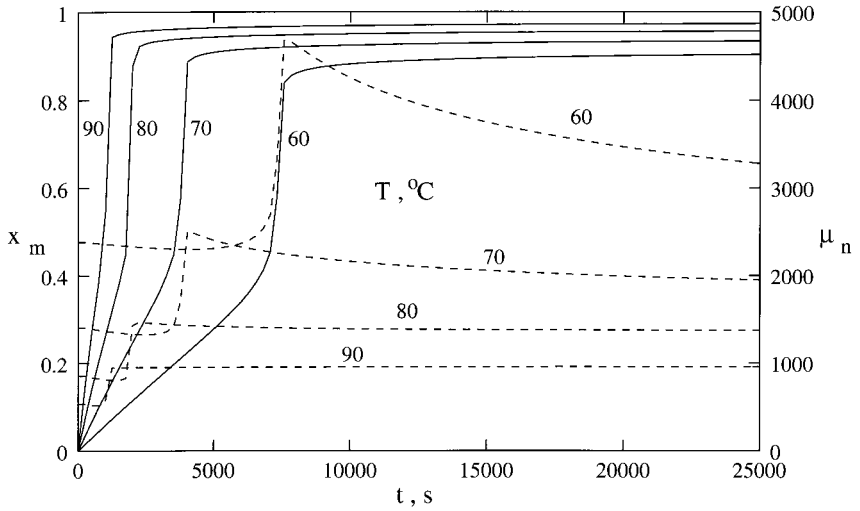

Figure 2 $x_m(t)$ (solid) and $\mu_n(t)$ (dotted) for isothermal bulk polymerization of MMA using AIBN ($[I]_o$ = 25.8 mol/m^3).

found upon decreasing the value of this parameter. This check indicated that the simulation part of our code was free of errors and also provided results that could be used to explain optimal histories qualitatively. The next check was on the correctness of the optimization part of our program. From Figure 2, it is clear that if we use

$$x_{md} = 0.0134$$
$$\mu_{nd} = 2365$$
$$60°\text{C} \le T(t) \le 90°\text{C} \qquad (14)$$

the optimal temperature history would be isothermal at 60°C (any higher temperature would give lower values of μ_{nf} while simultaneously giving higher x_{mf}). Also, under these isothermal conditions, the value of t_f would be 230.77 s. Similarly, for

$$x_{md} = 0.4926$$
$$\mu_{nd} = 532.16$$
$$60°\text{C} \le T(t) \le 90°\text{C} \qquad (15)$$

the optimal $T(t)$ would be isothermal at 90°C (see Fig. 2), with t_f = 969.67 s (any lower temperature would lead to higher values of μ_{nf} while simultaneously leading to lower x_{mf}). The optimization problems described in eqs. (14) and (15) were solved using the GA computer code (using the parameters of Table IV), and, in both cases, the expected optimal temperature histories were obtained [in eight generations for eq. (14) and three generations for eq. (15)]. A similar check was made for the computer code using Pontryagin's principle with the first order control vector iteration method (P1). The starting guess for this technique was $T^{(o)}$ = 90°C [for eq. (14)] and $T^{(o)}$ = 60°C [for eq. (15)]. Again, the expected isothermal optimal histories were obtained in two and eight iterations [for eqs. (14) and (15), respectively]. These checks gave confidence on both our computer codes, GA and P1.

The optimization program using GA was now run for

$$x_{md} = 0.94$$
$$\mu_{nd} = 1800$$
$$60°\text{C} \le T(t) \le 90°\text{C} \qquad (16)$$

These values are quite close to those used by Vaid and Gupta,[34] as well as other workers, and are being used as reference values to illustrate the working of GA. Figure 3 shows how the optimal temperature history (the best for each generation) evolves over generations. Very little improvement takes place after about 12 generations, and so results for $N_g > 12$ are not shown. The CPU time for generating these results was 15.8 s on a DEC 3000 αxp. The variation of μ_n and x_m with time, using the optimal temperature history (for N_g = 12) shown as GA15 (15 indicating $\Delta u_{\min}$ and $\Delta u_{\max}$ of −15 and +15°C) in Figure 3, are shown in Figures 4 and 5 (by solid lines marked GA15). Some amount of oscillations are observed in the optimal temperature history (Fig. 3), which

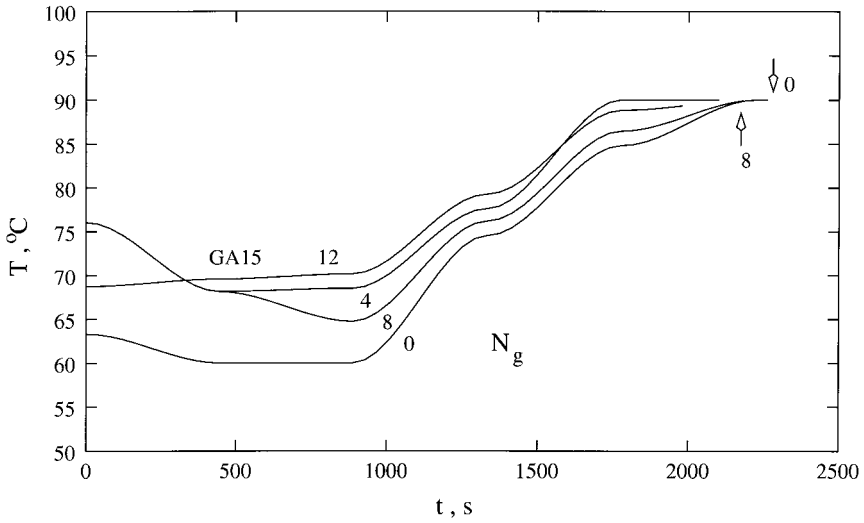

Figure 3 Evolution of temperature histories towards the optimal one, with generation number N_g corresponding to $x_{md} = 0.94$, $\mu_{nd} = 1800$ (for parameters of Table VII). Arrows indicate the end points of corresponding curves.

could be reduced by changing some of the parameters in Table VI (see later). Figure 6 compares the optimal history (curve GA15; same as for $N_g = 12$ in Fig. 3) with that obtained using Pontryagin's minimum principle (curve P1, obtained by starting with $T^{(o)} = 90°C$ and converging in about eight iterations). The values of the objective function I for the GA15 and the P1 cases are found to be 2008.36 and 2016.96, respectively. The two histories are also observed to be fairly close to each other. It may be noted[24,25,27–30] that both GA and P1 lead to near optimal solutions only and become very sluggish as the optimal history is approached. The agreement in Figure 6 is, thus, extremely good (perhaps fortuitously so). It is interesting to observe from Figure 3 and 4 that optimal operation requires relatively low temperatures (leading to relatively high values of μ_n; see Fig. 4), followed by a gradual increase in $T(t)$ (associated with some fall in μ_n) to its maximum value of 90°C. The value of μ_n builds up to its desired value by exploiting the gel effect near the end, this being exhibited as a sharp increase in $\mu_n(t)$ and $x_m(t)$ near $t \cong t_f$. The sudden increase in $\mu_n(t)$ to its final value of μ_{nd} is a characteristic of almost all optimal solutions obtained in our

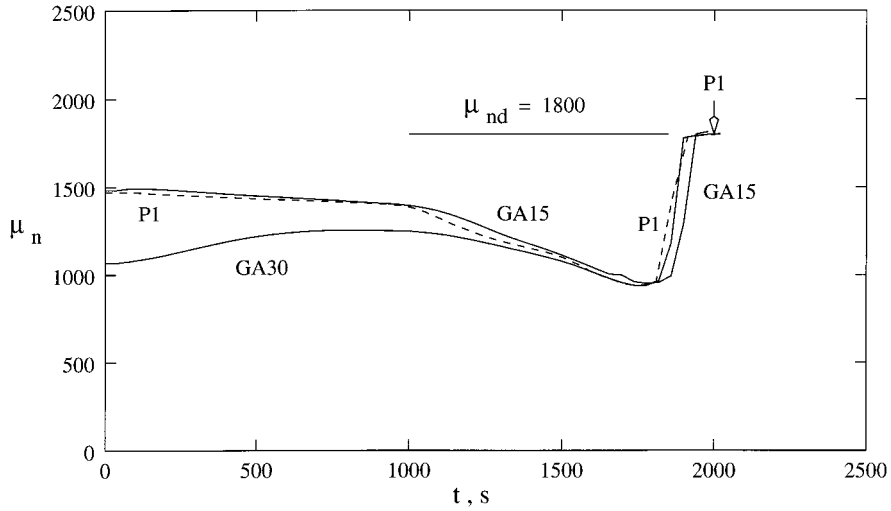

Figure 4 $\mu_n(t)$ corresponding to $T_{opt}(t)$ for the GA15 run, as well as for those corresponding to Figure 6.

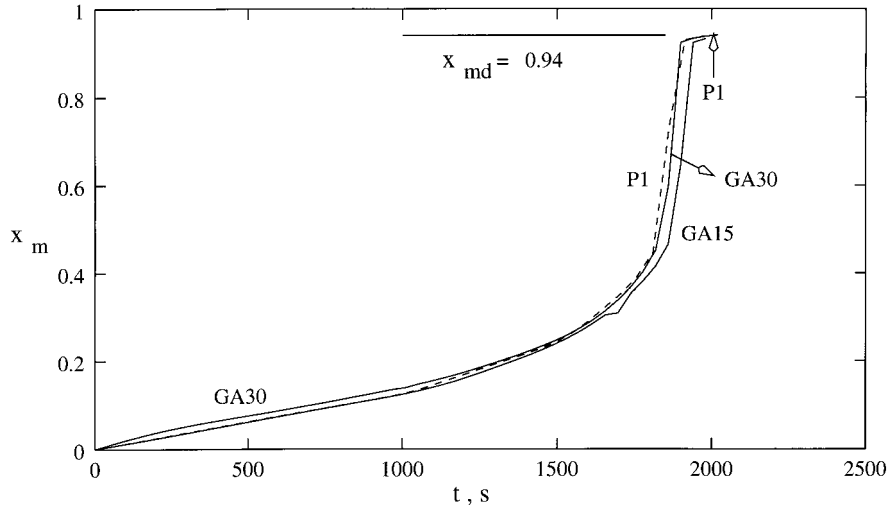

Figure 5 $x_m(t)$ corresponding to the GA15 run, as well as for those given in Figure 6.

study and emphasizes the need for model-based on-line optimizing control in the period prior to the onset of the gel effect.

Computations were carried out using Pontryagin's minimum principle (first order) for the conditions described in eq. (16), but using the initial guess $T^{(o)}(t)$, different than that used for generating Figures 4–6 (i.e., isothermal $T^{(o)}(t)$ different from 90°C). It was found that the (near) optimal temperature histories were very sensitive to the initial guess and that there was only a very narrow window of the initial guess for which converged solutions were obtained which were similar to GA15. A similar acute sensitivity to the initial guess history was also observed by Vaid and Gupta,[34] who used a similar algorithm but solved a slightly different optimization problem. In fact, we obtained different (sub-) optimal temperature histories on using different $T^{(o)}(t)$ outside of the narrow window. In each case, the x_{mf} and μ_{nf} were very close to their desired values, while the values of I differed slightly. This could be because of two possible reasons. First, the value of I_{opt} is relatively insensitive to $T_{\text{opt}}(t)$; and second, there could be several shallow, local minima, and P1 converges to (near) these, depending on the initial guess $T^{(o)}(t)$ provided. Which of these two causes leads to the ineffectiveness of the P1 technique is not clear; nor is this answer too important. However, GA is known[24,25] to reach the global optimum and is robust, so we believe that its solution is the true one. The P1 technique also converges to the solution provided by GA if we start from $T^{(o)} = 90$°C or use $T^{(o)}(t)$ somewhat similar (but not identical) to the optimal history provided by GA.

This drawback of the P1 technique can be overcome by the use of GA to first generate near optimal solutions that can be provided as initial guess to be improved upon by using P1. We believe that GA followed by P1 is a superior combination than the first order Pontryagin technique followed by the second order (P2) technique,[27–30] in which second order derivatives are required. Figure 7 shows the improvement of the optimal $T(t)$ using the GA15-P1 combination. The value of I of 2008.71 corresponding to GA15 is reduced to 1980.34 using the P1 technique. Similar improve-

Table VI Parameters Used for Reference Run

GA Parameters
$N_p = 100$
$N_{\text{str}} = 7$
$N_{ga} = 10$
$N_{\text{sim}} = 100$
$[u_{\min}, u_{\max}] = [60, 90]$; °C
$[\Delta u_{\min}, \Delta u_{\max}] = [-15, +15]$; °C
$p_c = 0.99$
$p_m = 0.000009$
$S = 0.2$
$t_{fo} = 4000$ s
$w_1 = w_2 = 2.5 \times 10^5$
In addition, the value of the parameter RS used[25] for generating binaries is 0.9.

Design Parameters
$x_{md} = 0.94$
$\mu_{nd} = 1800$
$[I]_o = 25.8$ mol/m^3

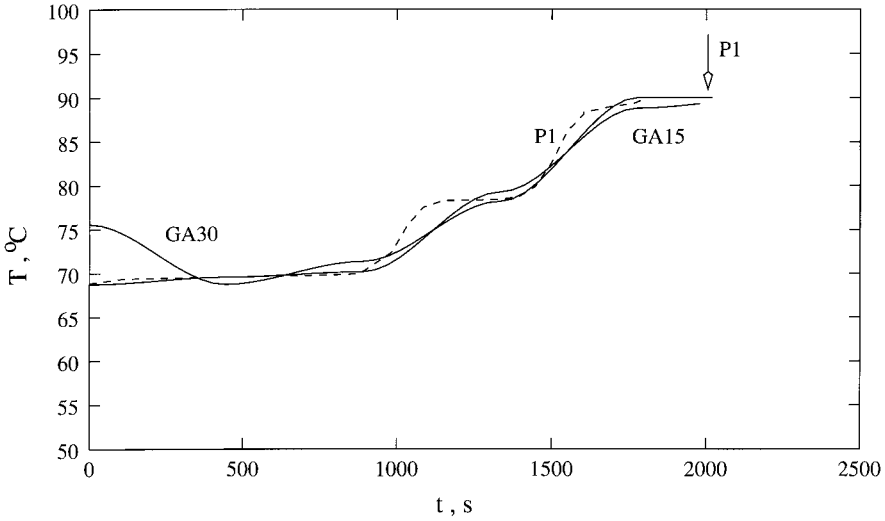

Figure 6 $T_{opt}(t)$ corresponding to the conditions of Figure 3 using the P1 (dotted) and GA (solid) techniques. GA15 corresponds to the reference run (Table VII), while GA30 corresponds to $[\Delta T_{min}, \Delta T_{max}] = \pm 30°C$ (all other parameters are the same as given in Table VII). Arrow indicates t_f for P1.

ments in the value of I have been found in other cases of GA + P1 tried in this study (detailed results can be provided on request).

We now study the effect of varying the parameters (Table VI) used in GA. Details of the parameters, which are varied one at a time, keeping all others at their reference values (Table VI), are given in Table VII. Figure 8 shows that in the initial region (low t), the optimal temperature history is somewhat sensitive to the number N_p of chromosomes in the population (curves 1 and 2). However, changing N_p could lead to oscillatory behavior in $T_{opt}(t)$, which needs to be dampened by changing some other parameter (e.g., Δu_{min}, Δu_{max}) simultaneously. In fact, the reference values of the parameters (run GA15) have been chosen such that the oscillations are minimized for this run. Similar oscillatory behavior is observed (curve 3, Fig. 8) in the initial region by increasing N_{str} from 7 (ref) to 14. It is clear that any change made to improve the accuracy of results leads to more oscillations in the initial region, and its effects need to be dampened out. A similar conclusion is obtained on studying curves 4 and 5 in

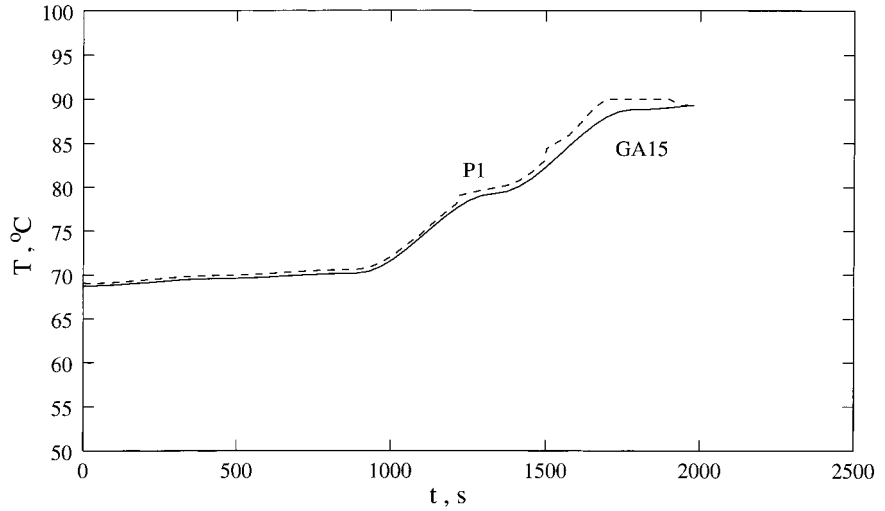

Figure 7 $T_{opt}(t)$ obtained with the P1 (dotted) technique using the optimal history from GA15 (solid) as an initial guess.

Table VII Some Details Corresponding to $T(t)$ Shown in Figures 8–13

Curve No.	Parameter Varied	Parameter Value (Ref. Value)	I_{opt}	N_g[a]	Fig. No.
GA15	—	Table 6	2008.36	12	8
1	N_p	50 (100)	2076.49	9	8
2	N_p	200 (100)	1953.89	15	8
3	N_{str}	14 (7)	1959.63	18	8
4	N_{ga}	20 (10)	2065.29	13	9
5	N_{ga}	30 (10)	2191.00	10	9
6	p_m	10^{-5} (9×10^{-6})	2265.56	14	10
7	p_c	0.98 (0.99)	2101.24	14	10
8	N_{sim}	80 (100)	2128.62	16	10
9	RS	0.6 (0.9)	1946.64	17	10
10	ΔT_{min} ΔT_{max}	±20°C (±15°C)	2021.63	7	11
11	ΔT_{min} ΔT_{max}	±30°C (±15°C)	2020.52	7	11
12	S	0.4 (0.2)	2141.61	10	11
13	x_{md}	0.95 (0.94)	2384.44	16	12
14	μ_{nd}	1600 (1800)	1850.98	17	13
15	μ_{nd}	2000 (1800)	2294.14	17	13
16	$[I]_o$	15.48 (25.8)	1629.82	6	13

[a] For achieving convergence.

Figure 9 and curve 8 in Figure 10. As N_{ga} is increased, $T_{opt}(t)$ oscillates considerably, to the extent that I_{opt} worsens. The effect of increasing the mutation probability is similar. Decreasing the crossover probability from 0.99 to 0.98 (curve 7, Fig. 10) does not lead to oscillations, but worsens I_{opt} slightly. The effects of decreasing N_{sim} and changing RS are also shown (curves 8 and 9) in Figure 10.

Figure 11 shows the effect of varying the parameter characterizing one of the adaptations of the conventional GA, namely, the use of Δu_{min} and Δu_{max} as constraints. These were introduced to dampen oscillations in $T_{opt}(t)$, as well as to

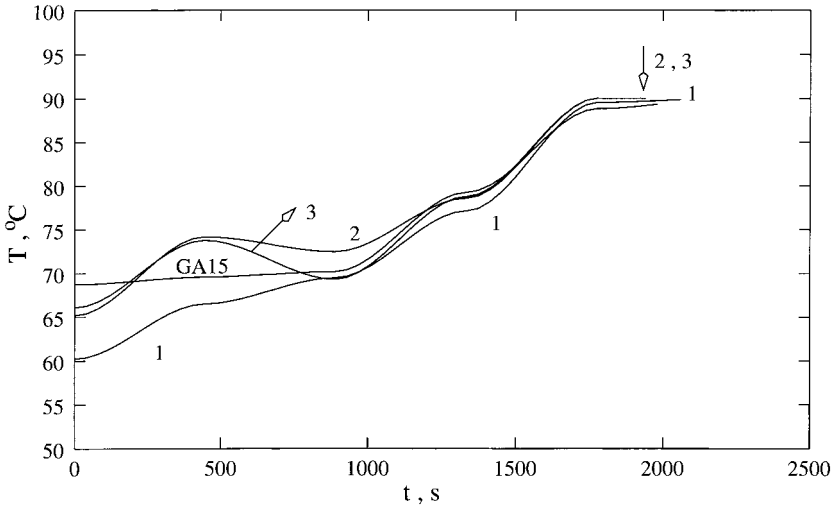

Figure 8 Effect of varying N_p and N_{str} on the optimal temperature histories. Curve 1: $N_p = 50$. Curve 2: $N_p = 200$. Curve 3: $N_{str} = 14$. Results for the reference run (GA15) also shown for comparison.

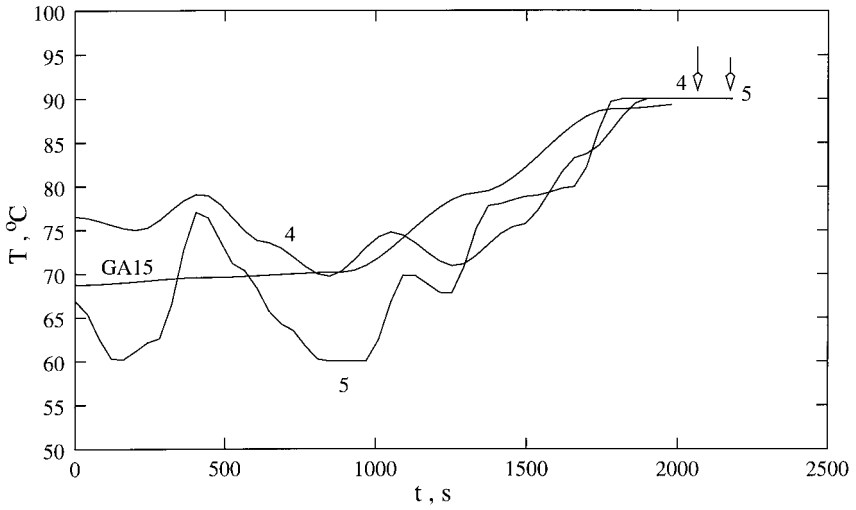

Figure 9 Effect of varying N_{ga} on the optimal temperature history. Curve 4: $N_{ga} = 20$. Curve 5: $N_{ga} = 30$.

ensure implementability of the optimal history in industrial systems. The actual values of ΔT_{min} and ΔT_{max} to be used should really be decided by the heat transfer limitations of the reactor, but these have been considered as parameters and chosen somewhat arbitrarily here to study their effect. It is observed that increasing the range of ΔT from ± 15 to ± 30°C leads, as expected, to more oscillations and to a worsening of I_{opt}. It is interesting to compare curve 11 (for $-30 \leq \Delta T \leq 30$°C; i.e., no constraint is operative on the temperature of a neighboring point, except 60°C $\leq T \leq$ 90°C), with the results from the P1 technique [with $T^{(o)}(t) = 90$°C], in which no constraint on the temperatures of neighboring points are operative. Figure 6 shows that curve 11 (renamed GA30) does not compare as well with curve P1 quantitatively, as does the GA15 results due to the oscillations present in GA30. Use of a damping mechanism through ΔT_{min} and ΔT_{max} thus appears justified.

Figure 11 also shows (curve 12) the effect of increasing the safety factor S, a parameter reflecting another adaptation we have made in the conventional GA. Increasing S leads to a larger domain in which crossovers are permitted and slows down the rate of convergence (note that GA, too, becomes sluggish as the optimal history is

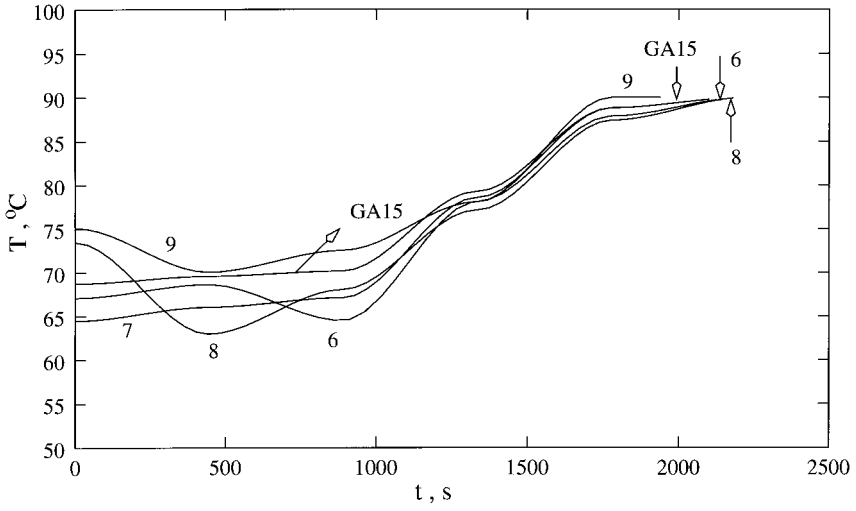

Figure 10 Effect of varying p_m, p_c, N_{sim}, and RS on the optimal temperature history. Curve 6: $p_m = 10^{-5}$. Curve 7: $p_c = 0.98$. Curve 8: $N_{sim} = 80$.

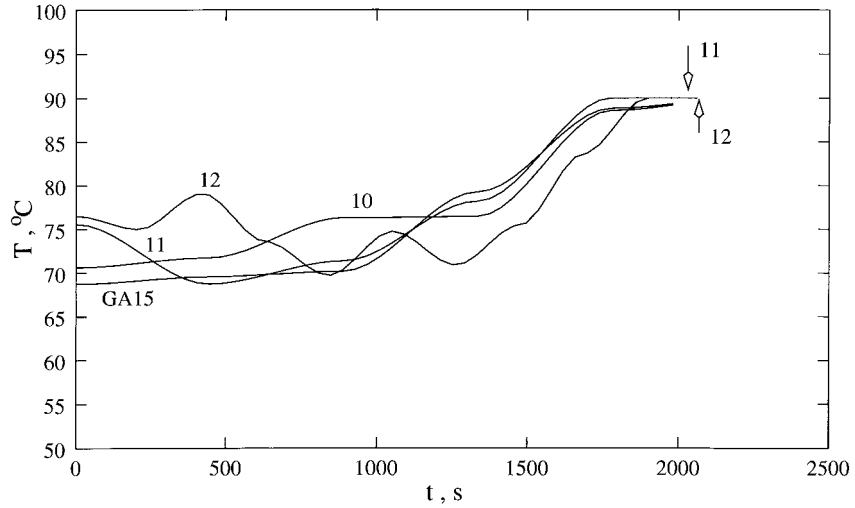

Figure 11 Effect of varying $(\Delta T_{\min}, \Delta T_{\max})$ and S on the optimal temperature history. Curves 10 and 11: $(\Delta T_{\min}, \Delta T_{\max}) = \pm 20$ and ± 30°C, respectively. Curve 12: $S = 0.4$.

approached, and the results in Figs. 8–11 are all near optimal in that sense).

The general conclusion from this parametric sensitivity study is that we need to experiment with the several parameters to obtain good, near-optimal u-histories with GA. In fact, one can carry out such a study to establish some general rules for the choice of the parameters, but this was not the focus of the present work. Since the histories are global (near) optimal solutions, we can follow up GA with the first order Pontryagin (P1) technique to get good final results. This combination exploits the best features of both these techniques.

Figures 12 and 13 show the effect of varying the design variables x_{md}, μ_{nd}, and $[I]_o$. Figure 12 (curve 13) shows that somewhat lower initial temperatures and slower rates of rise of $T(t)$ are required to obtain higher final values of the monomer conversion if we wish to keep μ_{nd} unchanged. The presence of oscillations in $T_{\text{opt}}(t)$ indicates that the reference values of the parameters used are not appropriate to generate the results for this case and need to be retuned if we wish to have better results. Figure 13 (curves 14 and 15) shows how the increase of $T_{\text{opt}}(t)$ should be delayed to give higher μ_{nf} products. Figure 14 shows the delayed gel effect helping achieve higher μ_{nf} products. The effect of decreasing the initiator loading

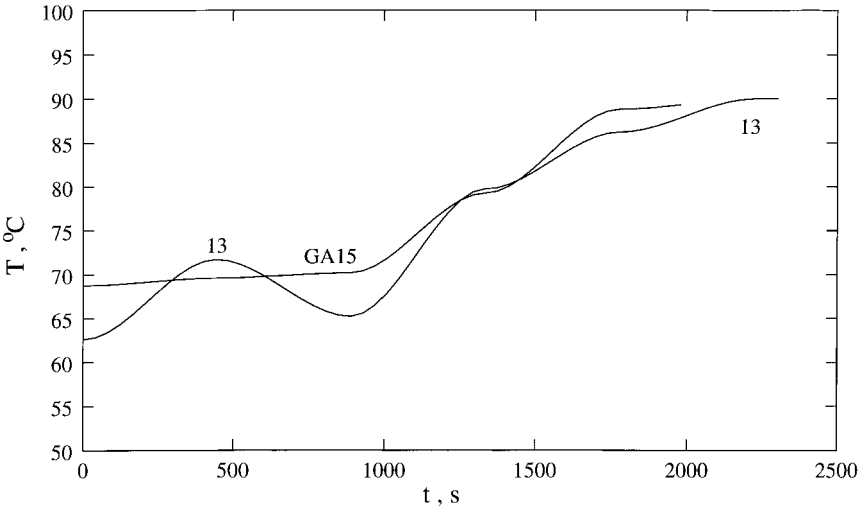

Figure 12 Effect of varying x_{md} on the optimal temperature histories. Curve 13 corresponds to $x_{md} = 0.95$.

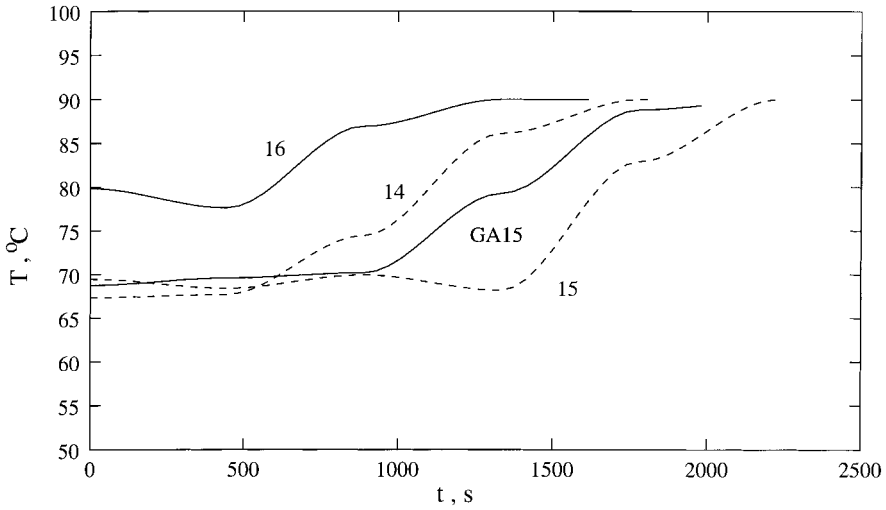

Figure 13 Effect of varying μ_{nd} and $[I]_o$ on the optimal temperature histories. Curves 14 and 15: μ_{nd} = 1600 and 2000, respectively. Curve 16: $[I]_o$ = 15.48 mol/m^3.

$[I]_o$ is also shown in Figure 13 (curve 16). Higher temperatures are necessary with lower $[I]_o$ to speed up the reaction so that t_f is minimized.

The general trends observed in all these cases is that optimal temperature histories for MMA polymerization are such that, initially, we have almost constant μ_n. This is followed by a period during which μ_n decreases (as T goes up). Finally, the gel effect occurs, which leads to a relatively rapid increase in x_m and μ_n to their desired values. The temperatures in the pre-gel effect region are quite important, particularly since rapid changes in T after the onset of the gel effect are not easy to implement. This points out the need for using model-based on-line optimizing control. It is difficult to predict the qualitative trends of $T_{\text{opt}}(t)$ intuitively using the isothermal results shown in Figure 2, and this emphasizes the importance of such quantitative studies.

The variation of the polydispersity index (PDI; see the nomenclature section) of the polymer with time, under optimal conditions (GA15), is shown in Figure 15. The final value of the PDI is observed to be substantially lower than that of polymer produced under isothermal conditions, which is a blessing in disguise, since reduction of the PDI was not envisaged in our optimization problem [eq. (6)]. There appears to be some controversy in the litera-

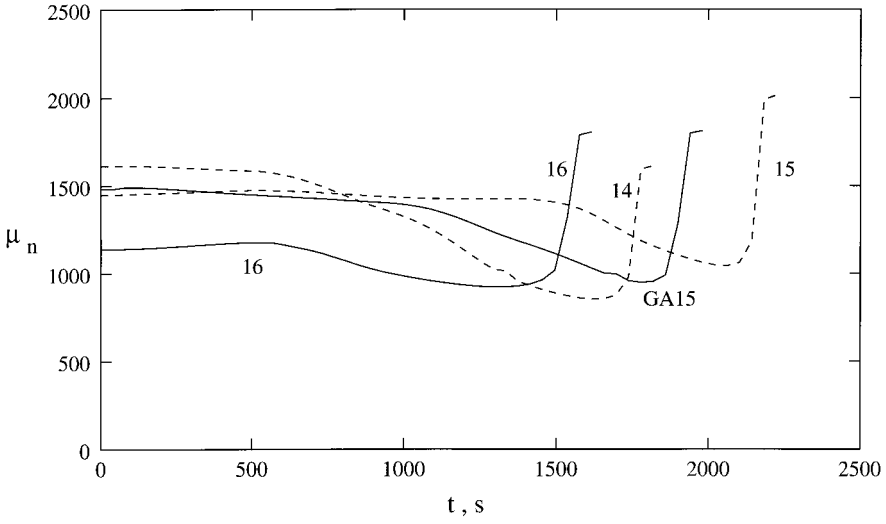

Figure 14 $\mu_n(t)$ corresponding to the optimal temperature histories given in Figure 13.

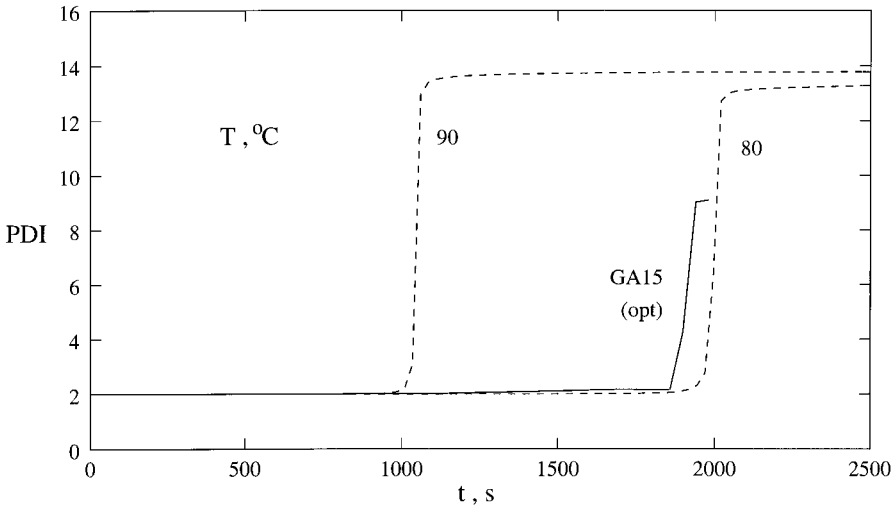

Figure 15 Variation of the polydispersity index (PDI) with time. The solid curve represents the PDI corresponding to the GA15 run, while the dotted curves correspond to isothermal polymerizations at 80 and 90°C.

ture regarding whether the minimum time problem ensures, simultaneously, minimum PDI.[34] Our results indicate substantial lowering of the PDI.

CONCLUSIONS

A robust optimization technique, genetic algorithm, has been used in this study to obtain global optimal temperature histories for MMA polymerization. These can be improved further by using the first order Pontryagin method. The technique can easily be used for on-line optimizing control of experimental reactors.

NOMENCLATURE

a	lower limit of u
b	upper limit of u
D_n	dead polymer molecule having n repeating units
f	initiator efficiency
$\mathbb{F}$	fitness function [eq. (11)]
I	objective function
I	moles of initiator at any time t (mol)
$[I]_o$	initial molar concentration of initiator (mol m^{-3})
k_d, k_i, k_f, k_p k_s, k_{tc}, k_{td}	rate constants for the reactions in Table I at any time t (s^{-1} or m^3 mol^{-1} s^{-1})
$l^{(i)}_{N_{\text{chr}}}$	i^{th} chromosome in population
M	moles of monomer in liquid phase (mol)
M_n	number average molecular weight $= (MW_m)(\lambda_1 + \mu_1)/(\lambda_o + \mu_o)$ (kg mol^{-1})
M_w	weight average molecular weight $= (MW_m)(\lambda_2 + \mu_2)/(\lambda_1 + \mu_1)$ (kg mol^{-1})
(MW_I), (MW_m), (MW_s)	molecular weights of pure primary radicals, monomer, and solvent (kg mol^{-1})
N_{chr}	total number of binary digits in chromosome $= N_{\text{ga}}N_{\text{str}}$
N_g	generation number
N_{ga}	number of u values GA generates
N_p	number of chromosomes in the population
N_{sim}	number of u values after interpolation
N_{str}	number of binary digits representing each of the N_{ga} control variables
$\boldsymbol{p}$	vector representing the model parameters θ_f, θ_p, θ_t

p_c	probability for crossover
p_m	probability for mutation
PDI	polydispersity index ($=M_w/M_n$)
P_n	growing polymer radical having n repeat units
R	primary radical
RS	parameter in random generator code
S	moles of solvent in liquid phase (mol)
S	safety factor
S	solvent radical
t	time (s)
t_f	total (final) reaction time (s)
t_{fo}	initially assumed value for t_f (s)
$T^{(o)}(t)$	initial guess temperature history in Pontryagin's technique
$T(t)$	temperature at time t (K)
$\boldsymbol{u}$	control vector (scalar, u, in this work)
$u^{(i)}(j)$	value of control variable at the end of j^{th} time interval in the i^{th} chromosome
$u_{\min}$, $u_{\max}$	lower and upper bounds on the control variable
$\Delta u_{\min}$, $\Delta u_{\max}$	minimum and maximum changes allowed between neighboring values of u
$U^{(i)}(j)$	value of control variable at the end of j^{th} (interpolated) time interval in the i^{th} chromosome
V_l	volume of liquid at time t (m^3)
w_1, w_2	weightage factors
$\boldsymbol{x}$	vector representing state variables
$x_m(t)$	monomer conversion (molar) at time t [eq. (7a)]

Greek Letters

ξ_{I3}, ξ_{13}	parameters in gel effect model (defined in Seth and Gupta[19])
ζ_m, ζ_{m_1}	net monomer added to the reactor, as defined in Seth and Gupta[19]
θ_f, θ_p, θ_t	adjustable parameters in the model for cage, gel, and glass effects, respectively (m^3 mol^{-1}, s, s)
λ_k	kth (k = 0, 1, 2, $\cdots$) moment of live (P_n) polymer radicals $\equiv \sum_{n=1}^{\infty} n^k P_n$ (mol)
μ_k	kth (k = 0, 1, 2, $\cdots$) moment of dead (D_n) polymer chains $\equiv \sum_{n=1}^{\infty} n^k D_n$ (mol)
μ_n	number average chain length at time $t \equiv (\lambda_1 + \mu_1)/(\lambda_o + \mu_o)$
μ_w	weight average chain length at time $t \equiv (\lambda_2 + \mu_2)/(\lambda_1 + \mu_1)$
ψ	free volume parameter (defined in Seth and Gupta[19])

Subscripts/Superscripts

d	desired value
f	final value (at $t = t_f$)
min	minimum
o	initial value
opt	optimal value

The authors would like to thank Professor Kalyanmoy Deb, Department of Mechanical Engineering, IIT Kanpur, for providing us the computer code, SGA, and for having several useful discussions. Also, we appreciate the partial support of this study through a grant from the Department of Science and Technology, New Delhi, as well as through Grant No. 22 (0232)/93/EMR-II of the Council of Scientific and Industrial Research, New Delhi, India.

REFERENCES

1. V. E. Trommsdorff, H. Kohle, and P. Lagally, *Makromol. Chem.,* **1,** 169 (1947).
2. R. G. W. Norrish and R. R. Smith, *Nature,* **150,** 336 (1942).
3. K. F. O'Driscoll, *Pure Appl. Chem.,* **53,** 617 (1981).
4. A. E. Hamielec, *Chem. Eng. Commun.,* **24,** 1 (1983).

5. D. Achilias and C. Kiparissides, *J. Appl. Polym. Sci.,* **35,** 1303 (1988).
6. D. S. Achilias and C. Kiparissides, *Macromolecules,* **25,** 3739 (1992).
7. I. Mita and K. Horie, *J. Macromol. Sci., Rev. Macromol. Chem. Phys.,* **C27,** 91 (1987).
8. J. N. Farber, in *Handbook of Polymer Science and Technology,* Vol. 1, N. P. Cheremisinoff, Ed., Dekker, New York, 1989, p. 429.
9. B. M. Louie and D. S. Soong, *J. Appl. Polym. Sci.,* **30,** 3707 (1985).
10. A. Faldi, M. Tirrell, and T. P. Lodge, *Macromolecules,* **27,** 4176 (1994).
11. A. Faldi, M. Tirrell, T. P. Lodge, and E. von Meerwall, *Macromolecules,* **27,** 4184 (1994).
12. G. T. Russell, R. G. Gilbert, and D. H. Napper, *Macromolecules,* **25,** 2459 (1992).
13. G. T. Russell, R. G. Gilbert, and D. H. Napper, *Macromolecules,* **26,** 3538 (1993).
14. P. A. Clay and R. G. Gilbert, *Macromolecules,* **28,** 552 (1995).
15. W. Y. Chiu, G. M. Carratt, and D. S. Soong, *Macromolecules,* **16,** 348 (1983).
16. G. V. Schulz and G. Harborth, *Makromol. Chem.,* **1,** 106 (1947).
17. S. T. Balke and A. E. Hamielec, *J. Appl. Polym. Sci.,* **17,** 905 (1973).
18. A. B. Ray, D. N. Saraf, and S. K. Gupta, *Polym. Eng. Sci.,* **35,** 1290 (1995).
19. V. Seth and S. K. Gupta, *J. Polym. Eng.,* **15,** 283 (1996).
20. T. Srinivas, S. Sivakumar, S. K. Gupta, and D. N. Saraf, *Polym. Eng. Sci.,* **36,** 311 (1996).
21. V. Dua, D. N. Saraf, and S. K. Gupta, *Polym. Eng. Sci.,* **59,** 749 (1996).
22. T. J. Tulig and M. V. Tirrell, *Macromolecules,* **14,** 1501 (1981).
23. J. H. Holland, *Adaptation in Natural and Artificial Systems,* Univ. Michigan Press, Ann Arbor, 1975.
24. D. E. Goldberg, *Genetic Algorithms in Search, Optimization and Machine Learning,* Addison-Wesley, Reading, MA, 1989.
25. K. Deb, *Optimization For Engineering Design: Algorithms and Examples,* Prentice Hall of India, New Delhi, 1995.
26. P. F. Lyons and A. V. Tobolsky, *Polym. Eng. Sci.,* **10,** 1 (1970).
27. W. H. Ray, *Advanced Process Control,* McGraw-Hill, New York, 1981; Butterworths, New York, 1989.
28. W. H. Ray and J. Szekeley, *Process Optimization,* Wiley, New York, 1973.
29. A. E. Bryson and Y. C. Ho, *Applied Optimal Control,* Blaisdell, Waltham, MA, 1969.
30. L. Lapidus and R. Luus, *Optimal Control of Engineering Processes,* Blaisdell, Waltham, MA, 1967.
31. M. E. Sachs, S. Lee, and J. A. Biesenberger, *Chem. Eng. Sci.,* **27,** 2281 (1972).
32. J. N. Farber and R. L. Laurence, *Chem. Eng. Commun.,* **46,** 347 (1986).
33. S. K. Gupta, *Numerical Methods For Engineers,* New Age Intl. Publ., New Delhi, 1995.
34. N. R. Vaid and S. K. Gupta, *Polym. Eng. Sci.,* **31,** 1708 (1991).
35. A. K. Ray and S. K. Gupta, *Polym. Eng. Sci.,* **26,** 1033 (1986).

Received April 13, 1996
Accepted July 25, 1996